Wireless Pers Commun (2008) 45:131–143
DOI 10.1007/s11277-007-9404-y

A Joint OFDM Channel Estimation and ICI Cancellation for Double Selective Channels

Qi Jiang · Joachim Speidel · Chunming Zhao

Published online: 2 October 2007

Abstract Orthogonal frequency division multiplexing (OFDM) systems suffer significantly from inter-carrier interference (ICI) caused by double selective channels. In this paper, we develop a two-stage hybrid channel estimation and ICI cancellation structure for OFDM. The double selective channels are approximated by an improved Basis Expansion Model (BEM), which is more accurate than the conventional BEM when the normalized Doppler frequency is smaller than one. Based on this improved model, a new ICI cancellation scheme is proposed to reduce ICI impact. Simulation results show that the framework performs well.

Keywords Inter-carrier interference (ICI) · Double selective channels · BEM · Channel estimation · ICI cancellation

1 Introduction

Orthogonal frequency division multiplexing (OFDM) [1] is one of the most practical technologies for high data rate transmission over frequency selective fading channels. In mobile communications, the double selective channels, whose time domain channel impulse response varies with time rapidly, destroy the orthogonality of OFDM, and thus give rise to the inter-carrier interference (ICI) among all the subcarriers.

Different approaches to reduce the ICI have been investigated widely, mainly time- or frequency-domain equalization [2–4] and ICI cancellation [5]. However, the time-domain channel information with high reliability must be provided firstly. Several approaches of modeling time-varying channels are available [6–10]. Prior to [9,10], a more general basis expansion model (BEM) for double selective channels was derived in [6,7].

Q. Jiang (✉) · J. Speidel
Institute of Telecommunications, University Stuttgart, Stuttgart, Germany
e-mail: qi@inue.uni-stuttgart.de

J. Speidel
e-mail: joachim.speidel@inue.uni-stuttgart.de

Q. Jiang · C. Zhao
National Mobile Communications Research Lab, Southeast University, Nanjing, China

Based on the BEM, we basically only need to estimate a limited number of BEM coefficients, which is more realistic and easier to handle than obtaining the complete time domain channel impulse response, so we can use the parsimonious parameters and coefficients to rebuild the whole time domain double selective channels. The beauty of using BEM also lies in the design of the equalization and ICI cancellation algorithms, in that it allows us to reduce a large design problem into a small one, only concerning the BEM coefficients of the channels [4,6].

For double selective channel estimation, a training sequence is usually used. A time-domain optimal training structure for block transmissions has been designed in [7]. A frequency domain OFDM pilot-assisted channel estimation is also proposed in [11]. However, in [7] and [11], the frequency parameter ω_q is set to a multiple of $2\pi/K(K$ is the BEM observation window length), which will reduce the accuracy of BEM channel model when $f_{\max} K T_S < 1$, where $f_{\max}$ is the maximum Doppler spread and T_S is the sampling interval. In this paper, we present a modified BEM to increase estimation accuracy firstly. Furthermore, we introduce a new block-type OFDM channel estimation method, which overcomes the non-full rank problem in [11] while calculating the BEM coefficients. To this end, we adopt a new ICI cancellation scheme that will use the information from the channel estimation. According to the simulation results, the combined receiver can provide a good performance in both channel estimation and interference cancellation of the OFDM systems.

The organization of the rest paper is as follows. Section 2 introduces the OFDM system and the modified Basis Expansion Model. Section 3 describes the pilot-assisted channel estimation based on the modified BEM. In Sect. 4, we propose a new ICI cancellation structure with the support from the BEM coefficients. Simulation results of mean square error (MSE) and bit error rate (BER) are presented in Sect. 5. The final conclusions are given in Sect. 6.

Notation: We use upper (lower) bold face letters to denote matrices (column vector). Superscripts $(\cdot)^H$, $(\cdot)^*$ and $(\cdot)^+$ represent Hermitian, conjugate and pseudo inverse, respectively. We reserve $E_x\{\cdot\}$ for expectation value with respect to the random variable x within the brackets. $\otimes$ stands for Kronecker product, $\lceil\cdot\rceil$ for integer ceiling, $\lfloor\cdot\rfloor$ for integer floor, $\angle$ for the argument of a complex number. $\mathbf{I}_N$ denotes the identity matrix of size N and diag[$\mathbf{x}$] is a diagonal matrix with vector $\mathbf{x}$ on its diagonal. The discrete Fourier transform (DFT) matrix of size $N \times N$ is given by $[\mathbf{F}]_{m,k} = e^{(-j2\pi mk/N)/\sqrt{N}}(m, k \in 0, \ldots, N-1)$.

2 System and Channel Model

In this section, we first present our improvement on Basis Expansion Model (BEM). Then we introduce the OFDM system based on this modified double-selective channel models.

2.1 Double-Selective Channel Models

First we consider the random variation in one multipath l, of a multipath time variant mobile radio channel in [6,8] and [12]

$$h(t;l) = \sum_{q=1}^{Q} c_q(l) e^{j\phi_q} \exp\left\{ j2\pi f_{\max}\left(\cos\frac{2\pi q}{Q}\right) t\right\} \tag{1}$$

Here c_q is the amplitude of the qth basis, $f_{\max}$ is the maximum Doppler-frequency and ϕ_q is a uniformly distributed random variable in $[0, 2\pi]$. For sufficient large Q, the amplitude of (1) approximates a Rayleigh probability density function. After sampling the time domain channel impulse response at $t = nT_S$, we obtain

$$h(n;l) = \sum_{q=1}^{Q} c_q(l) e^{j\phi_q} \exp\left\{ j2\pi f_{\max} T_S \left(\cos \frac{2\pi q}{Q} \right) n \right\}$$
$$= \sum_{q=1}^{Q} \bar{h}_{q,l} \exp\left(j\omega_q n \right) \quad (2)$$

$$\text{where } \bar{h}_{q,l} := c_q(l) e^{j\phi_q} \text{ and } \omega_q = 2\pi f_{\max} T_S \cos(2\pi q/Q)$$

In [6,13] and [14], it is shown that the maximum Doppler diversity order equals the number of bases $(Q+1)$ for time-selective frequency-flat channels. Then in [7,15], a Basis Expansion Model (BEM) with two-dimensional diversity order (L+1)(Q+1) is proposed for the double-selective channel. Assuming the BEM observation window length is K, this BEM model is able to accurately model the discrete time-varying impulse response of tap l in parsimonious finite parameters as follows:

$$h^{BEM}(n;l) = \sum_{q=0}^{Q} h_{q,l}^{BEM} e^{j\omega_q n}, n \in [0, N-1], l \in [0, L]$$
$$\text{where } \omega_q := \frac{2\pi(q - Q/2)}{K}; L := \left\lceil \frac{\tau_{\max}}{T_S} \right\rceil; Q = 2\lceil f_{\max} K T_S \rceil \quad (3)$$

We see that the BEM channel expression for tap l is quite similar to (2). The main differences are as follows:

(D1) The model in (3) confirms the value of Q, which is the order of the double selective channel in one multipath. Then the factor $\cos(2\pi q/Q)$ is simplified with factor $(q-Q/2)/K$.

(D2) If we define the normalized maximum Doppler-spread $\xi := f_{\max} K T_S$, the ω_q in (3) is a multiple of $2\pi/K$ instead of $2\pi\xi/K$. That means in (3) we use the integer ceiling of ξ to rebuild the channel model when ξ is below one.

For both models, the coefficient ω_q dominates the variant velocity of the rebuild channel. Therefore the smallest ω_q in (3) is much bigger than the actual ω_q in (2) when ξ is below one. This will result in a mismatch between the real channel and the rebuild channel, and thus reduce the accuracy of BEM channel model. We propose a modified BEM based on (3), in which ω_q is returned back to ξ instead of the integer spacing when ξ is below one:

$$h(n;l) = \begin{cases} \sum_{q=-Q/2}^{Q/2} h_{q,l} e^{j\omega_q n}, 0 \le n \le K-1, \quad \text{if } \xi \ge 1 \quad \text{where} \quad Q = 2\lceil f_{\max} K T_S \rceil, \\ \xi = 1, \ \omega_q = 2\pi\xi q/K \\ \sum_{q=-Q/2}^{Q/2} h_{q,l} e^{j\omega'_q n}, 0 \le n \le K-1, \quad \text{if } \xi < 1 \quad \text{where} \quad Q = 2\lceil f_{\max} K T_S \rceil, \\ \xi = f_{\max} K T_S, \ \omega'_q = 2\pi\xi q/K \end{cases} \quad (4)$$

In Sect. 5, we will give the simulation results about the two types of BEM and it will turn out that the modified BEM model can achieve better performance when ξ is below one.

2.2 Block Transmission for OFDM

From [5], we know that the average channel impulse estimation of every multipath in time domain can be obtained by the IFFT of the channel frequency response on the pilot subcarriers. In order to get different $Q+1$ estimated average channel impulses of all $L+1$ multipaths in time-domain, we construct a block-form OFDM transmission with $Q+1$ sub-OFDM symbols. With the $(L+1)\times(Q+1)$ channel estimation resulting from least square (LS) algorithm and IFFT, the double-selective channels impulse response can be rebuilt by the modified Basis Expansion Model (BEM).

We assume that every sub-OFDM symbol consists of N sinusoidal carriers plus a length-P (equal to or larger than L) cyclic prefix to eliminate the inter-symbol interference (ISI). The window length of the modified BEM is $K=(Q+1)\times(N+P)$ and the modified BEM coefficients are defined as a column vector $[h_{-Q/2,0},\ldots,h_{-Q/2,L},\ldots h_{q,l},\ldots,h_{Q/2,0},\ldots,h_{Q/2,L}]^T$ with $h_{q,l}$ representing the qth BEM coefficient for the lth multipath. We use two arguments $[i,k]$ to describe the serial index in the whole OFDM symbol, so for the kth time instant in the ith sub-OFDM symbol of the lth multipath, the time-domain channel can be described as

$$h([i,k];l)=\sum_{q=-Q/2}^{Q/2} h_{q,l}\exp\{j\omega_q(k+P+i(N+P))\},\quad i\in[0,Q],\quad k\in[0,N-1] \tag{5}$$

We define $\mathbf{y}_i$ as the ith frequency response of the received sequence, $\mathbf{s}_i$ as the ith frequency domain symbol, $\mathbf{n}_i$ as the FFT-transformed additive white Gaussian noise. The data stream in the block OFDM system can be expressed as

$$\begin{aligned}\mathbf{y}_i&=\sum_{q=-Q/2}^{Q/2}\mathbf{H}_{q,i}\mathbf{D}_q\mathbf{s}_i+\mathbf{n}_i\\ \mathbf{H}_{q,i}&=\mathbf{F}\mathrm{diag}(\mathbf{b}_{q,i})\mathbf{F}^{\mathbf{H}},\ \mathbf{b}_{q,i}=[b_{q,i}(0),b_{q,i}(1),\ldots,b_{q,i}(N-1)]^T,\\ \mathbf{D}_q&=\mathbf{F}\mathrm{diag}[h_{q,0},\ldots,h_{q,L},0,\ldots,0]\mathbf{F}^{\mathbf{H}}\\ b_{q,i}(k)&=\exp\{j\omega_q(k+P+i(N+P))\},\quad i\in[0,Q],\quad k\in[0,N-1]\end{aligned} \tag{6}$$

3 The Pilot-assisted Channel Estimation

For channel estimation, we firstly estimate the BEM coefficients $h_{q,l}$ and then use them to rebuild the whole time-varying channels according to (5). Since the BEM channel coefficient $h_{q,l}$ is time invariant over the window length, channel estimation can be performed in $(Q+1)$ sub-OFDM symbols. From [4,5], we know that the main part of the inter-carrier interference on every subcarrier comes from the Q neighboring subcarriers. Besides, the research from [16] tells us the comb-type frequency pilot insertion will be a better way to get the channel information. Here M pilot clusters of length L_P are used as the pilot. In order to get all the $(L+1)$ multi-path time-domain impulse responses, M should be larger than L [16]. In each cluster, we use the similar method in [11] to insert pilots, which means setting two subcarriers for pilot data that are surrounded by the guard subcarriers (set to zero) of length $Q/2$ at each side. The total occupied guard subcarrier number in one pilot cluster is equal to $B_c(B_c=2Q)$. Although larger B_c can reduce the ICI effect on pilot subcarriers more significantly, we still need to set small $L_P(L_P=B_c+2)$ to avoid band redundancy. The detailed arrangement for one received frequency sub-OFDM symbol is shown in Fig. 1.

In Fig. 1, $y_{m,0}$ and $y_{m,1}$ represent the first and second pilot subcarrier in mth cluster respectively (The total observation sample vector for ith sub-OFDM symbol is $\mathbf{y}_i$). $\mathbf{s}_m^{(p)}$ represents

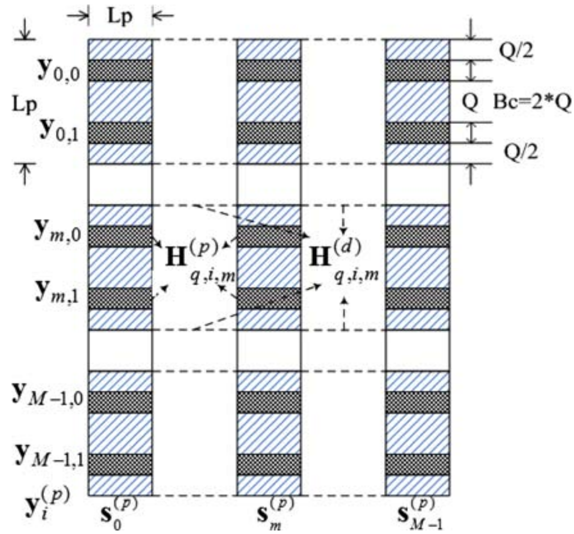

Fig. 1 Partition of matrix **H** in (4)

the *mth* pilot cluster with the length of L_P. The matrix $\mathbf{H}^{(p)}_{q,i,m}$ of size $(L_P - B_C) \times ML_P$, representing the grid parts in Fig. 1, addresses the parts of the frequency channel matrix related to the received pilot subcarriers. The $(L_P - B_C) \times (N - ML_P)$ matrix $\mathbf{H}^{(d)}_{q,i,m}$, representing the white parts in Fig. 1, contains the parts of the frequency channel matrix related to the information subcarriers.

We define $\mathbf{D}^{(d)}_q$ as an $(N - ML_P) \times (N - ML_P)$ matrix, which takes out all the non-pilot values from the $\mathbf{D}_q$ and arranges them in a diagonal matrix and $\mathbf{D}^{(p)}_q$ as a $ML_P \times ML_P$ diagonal matrix with pilot values on the diagonal. $\mathbf{y}_{m,i}$ represents the received vector of size $(L_P - B_C)$ on the corresponding pilot positions and $\mathbf{y}_i^{(p)} = [\mathbf{y}^T_{0,i}, \mathbf{y}^T_{1,i}, \ldots, \mathbf{y}^T_{M-1,i}]^T$. Then we can rewrite (6) as follows, here the superscript $(\cdot)^{(p)}$ denotes pilot-carrying subcarriers, with $\mathbf{F}^{(p)}_L$ and $\mathbf{F}^{(d)}_L$ standing for pilot and data positions in the first $L+1$ columns of the DFT matrix $\mathbf{F}$, respectively.

$$
\begin{aligned}
\mathbf{y}_{m,i} &= \sum_{q=-Q/2}^{q=Q/2} \mathbf{H}^{(p)}_{q,i,m}\mathbf{D}^{(p)}_q \mathbf{s}^{(p)} + \sum_{q=-Q/2}^{q=Q/2} \mathbf{H}^{(d)}_{q,i,m}\mathbf{D}^{(d)}_q \mathbf{s}^{(d)} + \mathbf{n}_{m,i} \\
\mathbf{y}_i^{(p)} &= \boldsymbol{\Xi}_i \mathbf{h} + \boldsymbol{\Psi}_i \mathbf{h} + \mathbf{n}_i^{(p)} \\
\mathbf{h} &= [h_{-Q/2,0}, \ldots, h_{-Q/2,L}, \ldots, h_{q,0}, \ldots, h_{q,L}, \ldots, h_{Q/2,0}, \ldots, h_{Q/2,L}]^{\mathbf{T}}
\end{aligned} \tag{7}
$$

$$
\begin{aligned}
\boldsymbol{\Xi}_i &= \begin{bmatrix} \mathbf{H}^{(p)}_{-Q/2,i,0} & \cdots & \mathbf{H}^{(p)}_{Q/2,i,0} \\ \vdots & \ddots & \vdots \\ \mathbf{H}^{(p)}_{-Q/2,i,M-1} & \cdots & \mathbf{H}^{(p)}_{Q/2,i,M-1} \end{bmatrix} \left(\mathbf{I}_{Q+1} \otimes (\mathbf{diag}(\mathbf{s}^{(p)})\mathbf{F}^{(p)}_L)\right) \\
\boldsymbol{\Psi}_i &= \begin{bmatrix} \mathbf{H}^{(d)}_{-Q/2,i,0} & \cdots & \mathbf{H}^{(d)}_{Q/2,i,0} \\ \vdots & \ddots & \vdots \\ \mathbf{H}^{(d)}_{-Q/2,i,M-1} & \cdots & \mathbf{H}^{(d)}_{Q/2,i,M-1} \end{bmatrix} \left(\mathbf{I}_{Q+1} \otimes (\mathbf{diag}(\mathbf{s}^{(d)})\mathbf{F}^{(d)}_L)\right)
\end{aligned} \tag{8}
$$

We combine the received $Q+1$ sub-OFDM data of one block in a column vector, and get

$$\mathbf{y}^{(p)} = \begin{bmatrix} \mathbf{y}_0^{(p)} \\ \vdots \\ \mathbf{y}_Q^{(p)} \end{bmatrix} = \boldsymbol{\Xi}\mathbf{h} + \boldsymbol{\Psi}\mathbf{h} + \mathbf{n} = \begin{bmatrix} \boldsymbol{\Xi}_0 \\ \vdots \\ \boldsymbol{\Xi}_Q \end{bmatrix} \cdot \mathbf{h} + \begin{bmatrix} \boldsymbol{\Psi}_0 \\ \vdots \\ \boldsymbol{\Psi}_Q \end{bmatrix} \cdot \mathbf{h} + \begin{bmatrix} \mathbf{n}_0^{(p)} \\ \vdots \\ \mathbf{n}_Q^{(p)} \end{bmatrix} \tag{9}$$

Then the LS and linear minimum mean square error (LMMSE) estimation is applied, respectively, which results in the time domain channel impulse response.

$$\hat{\mathbf{h}}_{LS} = \boldsymbol{\Xi}^{+}\mathbf{y}^{(p)} \tag{10}$$

$$\begin{aligned} \hat{\mathbf{h}}_{LMMSE} &= \mathbf{R}_h \boldsymbol{\Xi}^H (\boldsymbol{\Xi}\mathbf{R}_h \boldsymbol{\Xi}^H + \mathbf{R}_\Psi + \mathbf{R}_n^{(p)})^{-1}\mathbf{y}^{(p)} \\ \mathbf{R}_\Psi &= E_{\mathbf{h},\mathbf{s}^{(d)}}\{\boldsymbol{\Psi}\boldsymbol{\Psi}^H\},\ \mathbf{R}_n^{(p)} = E_{\mathbf{n}}^{(p)}\{\mathbf{n}^{(p)}\mathbf{n}^{(p)H}\} \end{aligned} \tag{11}$$

In order to get the $\mathbf{R}_h$, The BEM coefficients have the following statistical characteristics [7]:

(A1) The BEM coefficients $h_{q,l}$ are zero-mean, complex Gaussian random variables with $\sigma_{q,l}$.

(A2) The channel coefficients $h_{q,l}$ are independent and the correlation matrix $\mathbf{R}_h$ is a diagonal matrix with trace $\mathrm{tr}(\mathbf{R}_h) = 1$.

We also refer to another statistical condition of the BEM coefficients for time-selective channels [15].

(A3)

$$E\left\{\left|h_{-Q/2,l}\right|\right\} = \cdots = E\left\{\left|h_{0,l}\right|\right\} = \cdots = E\left\{\left|h_{Q/2,l}\right|\right\}.$$

Since we adopt the block transmission to obtain enough time domain channel estimates, the matrix $\boldsymbol{\Xi}$ has full rank except for poor channel situations.

4 ICI Cancellation Receiver Design

In the conventional receivers for the consistent carrier frequency offset (CFO), we can simply multiple the conjugate of the estimated exponential frequency offset to overcome the ICI influence. Every basis of the modified BEM is similar to a fixed channel amplitude multiplied by an exponent of the frequency offset. Hence, we combine the traditional consistent CFO cancellation method with the demodulation, and then propose a new receiver based on the modified BEM.

The ICI cancellation unit is separated into four stages. The detailed structure of the receiver is shown in Fig. 2. Since the processing of every sub-OFDM symbol is the same, we define $\hat{\mathbf{y}}$ as the time domain received data and omit the subscript "i" in the subsequent.

The first stage is to calculate the time-domain phase compensation factor $\hat{\xi}_{n,CP}$ and $\hat{\xi}_{n,CH}$, where n indicates the time instant and the subscripts "*CP*" and "*CH*" the estimated source. The second stage is to build the compensation Matrix $\tilde{\mathbf{D}}_{CP}$ and $\tilde{\mathbf{D}}_{CH}$ using the information from stage 1, where the $\tilde{\mathbf{D}}_{CP}$ and the $\tilde{\mathbf{D}}_{CH}$ are from the CFO estimation unit and the channel estimation unit, respectively. In stage 3 we use the windowed DFT-based method [17,18] to obtain the rotary demodulation coefficients. In the end, all the modules of the rotary channel coefficients are compared and the largest one is selected to fulfill the demodulation.

Assume the maximal Doppler frequency in one sub-OFDM symbol to be a consistent carrier frequency offset, a raw doppler frequency index $\hat{\xi}_{n,CP}$ can be estimated by the cyclic prefix (CP) [19].

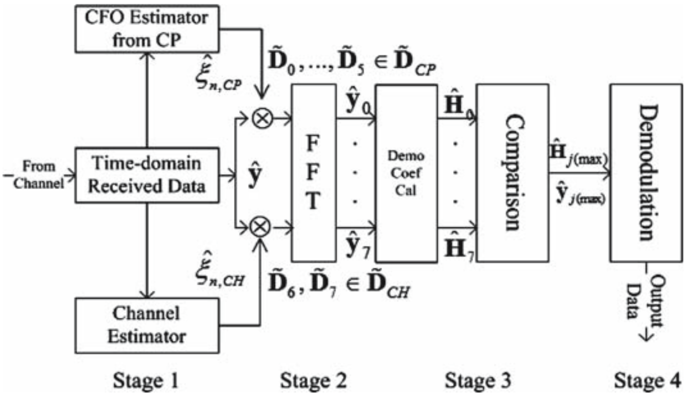

Fig. 2 ICI cancellation receiver

$$\hat{\xi}_{n,CP} = \frac{n}{N}\angle\left[\frac{1}{P-L}\sum_{a=L}^{P-L}\left(\frac{1}{Q+1}\sum_{i=0}^{Q} y_i^*(a)y_i(a+N)\right)\right], \quad n \in [0, N-1] \quad (12)$$

Here, N is the subcarriers number in a sub-OFDM symbol and P is the length of the CP. We set the $\hat{\xi}_{n,CP}$ to be equidistant at every time instant, so the Matrix $\tilde{\mathbf{D}}_{CP}$ can be described as

$$\tilde{\mathbf{D}}_{CP} = diag([1, \exp(j2\pi k_{CP}\hat{\xi}_{0,CP}/N), \ldots, \exp(j2\pi k_{CP}\hat{\xi}_{i,CP}/N), \ldots, \exp(j2\pi k_{CP}\hat{\xi}_{N-1,CP}/N)]) \quad (13)$$

k_{CP} is the multiplying factor like the q in BEM. On the consideration of computational complexity as well as the exponential structure of the BEM channel, k_{CP} can take from $\{-2, -1, -0.5, 0.5, 1, 2\}$. So we have six different $\tilde{\mathbf{D}}_{CP}$ to multiply the received data, which is numbered from $\tilde{\mathbf{D}}_0$ to $\tilde{\mathbf{D}}_5$.

The calculation method for the $\hat{\xi}_{n,CH}$ and $\tilde{\mathbf{D}}_{CH}$ are as follows. The $\hat{\xi}_{n,CH}$ is the accumulated phase discrimination between every two adjacent time-domain channel impulses. To reduce the number of the matrix $\tilde{\mathbf{D}}_{CH}$ and the complexity of the receiver, we only choose the two most powerful multipaths to calculate the $\hat{\xi}_{n,CH}$ and the $\tilde{\mathbf{D}}_{CH}$ (numbered from $\tilde{\mathbf{D}}_6$ to $\tilde{\mathbf{D}}_7$). Here $\hat{h}_{n,l}$ is the rebuilt channel impulse response by the BEM coefficients at time instant n from the two most powerful multipaths, l_1 and l_2.

$$\begin{aligned}
\hat{\xi}_{n,CH} &= \sum_{n=0}^{n}\angle(\hat{h}_{n+1,l}/\hat{h}_{n,l}) \\
\hat{h}_{n,l} &= \sum_{q=-Q/2}^{Q/2} h_{q,l}\exp(j\omega_q n), l \in [l_1, l_2] \quad l_1 = \mathop{\arg\max}_{l_1\in[0,L]}\left\{\sum_{q=-Q/2}^{q=Q/2} h_{q,l}\right\} \quad \text{and} \\
l_2 &= \mathop{\arg\max}_{l_2\in[0,L] \text{ and } l_2\neq l_1}\left\{\sum_{q=-Q/2}^{q=Q/2} h_{q,l}\right\}
\end{aligned} \quad (14)$$

$$\tilde{\mathbf{D}}_{CH} = diag([1, \exp(j2\pi\hat{\xi}_{1,CH}/N), \ldots, \exp(j2\pi\hat{\xi}_{i,CH}/N), \ldots, \exp(j2\pi\hat{\xi}_{N-1,CH}/N)]) \quad (15)$$

After stage 3, eight optional received data ($\hat{\mathbf{y}}_0$ to $\hat{\mathbf{y}}_7$) can be obtained after multiplying compensation matrices $\tilde{\mathbf{D}}_j$ ($\tilde{\mathbf{D}}_0, \ldots, \tilde{\mathbf{D}}_5$ from $\tilde{\mathbf{D}}_{CP}$ and $\tilde{\mathbf{D}}_6, \tilde{\mathbf{D}}_7$ from $\tilde{\mathbf{D}}_{CH}$) and FFT . We consider the $\hat{\mathbf{y}}_j$ as the new received frequency data (including the pilot and information) and use the simple DFT-based window [17,18] to obtain the rotary frequency domain channel coefficient. The DFT-based window frequency channel coefficients can be obtained by the following algorithm:

(1) After multiple the compensation matrix $\tilde{\mathbf{D}}_j$, the received data $\hat{\mathbf{y}}$ are rotated by the $\tilde{\mathbf{D}}_j$ and results in $\hat{\mathbf{y}}_j$. Use the Least Square (LS) method to get the rotary channel frequency response $\tilde{\mathbf{H}}^p_{LS,j}$ on the pilot subcarriers. The superscript "p" indicates the pilot position in every pilot cluster. Here $k \in [0, \ldots, M-1]$ and $p \in [1, 2]$.

$$\begin{aligned} \hat{\mathbf{y}}_j &= \mathbf{F}\tilde{\mathbf{D}}_j\hat{\mathbf{y}} = [\hat{y}_0, \ldots, \hat{y}_{N-1}]^{\mathbf{T}} \\ \tilde{\mathbf{H}}^p_{LS,j} &= [\tilde{H}^p_{LS,j}(0), \ldots, \tilde{H}^p_{LS,j}(M-1)]^T, \tilde{H}^p_{LS,j}(k) = \frac{\hat{y}_j(L_P k + 2p - 1)}{s(L_P k + 2p - 1)}; \\ & k \in [0, \ldots, M-1], p \in [1, 2] \end{aligned} \tag{16}$$

(2) An IFFT of size M is performed on $\tilde{\mathbf{H}}^p_{LS,j}$ and we calculate the average value $\tilde{h}_j(n)$ of two groups of channel time responses.

$$\begin{aligned} \tilde{h}^p_{LS,j}(n) &= \frac{1}{M}\sum_{m=0}^{M-1} \tilde{H}^p_{LS,j}(L_P m + 2p - 1)\exp(j2\pi\frac{mn}{M}), p \in [1, 2] \\ \tilde{h}_j(n) &= (\tilde{h}^1_{LS,j}(n) + \tilde{h}^2_{LS,j}(n))/2; n \in [0, 1, \ldots, M-1] \end{aligned} \tag{17}$$

(3) Use FFT of size N to obtain the final channel frequency response $\hat{H}_j(k)$ and select the information subcarriers based on $\hat{H}_j(k)$.

$$\begin{aligned} \hat{H}_j(k) &= \sum_{l=0}^{L-1} \tilde{h}_j(l)\exp(-j2\pi kn/N); k \in [0, \ldots, N-1] \\ \hat{\mathbf{H}}_j &= [\hat{H}_j(0), \ldots, \hat{H}_j(k), \ldots, \hat{H}_j(N-1)] \end{aligned} \tag{18}$$

Now from eight groups of optional $\hat{\mathbf{y}}_j$ and $\hat{\mathbf{H}}_j$, we need to find the one which is influenced by the ICI at least. Since the mean power of the channel impulse response is fixed in one sub-OFDM symbol, the effect of the time variation on the channel frequency matrix is to spread the power on the non-diagonal positions. If the $\left|\hat{H}_j(k)\right|$ is the maximal one of all eight optional objects after the steps above, the rotary process has congregated more power on the diagonal elements of the channel frequency matrix. Then, for all the information subcarriers, the related $\hat{y}_{j(\max)}(k)$ from $\hat{\mathbf{y}}_j$ and $\hat{H}_{j(\max)}(k)$ are picked out to do demodulation.

$$\hat{H}_{j(\max)}(k) = \arg\max_{j=0}^{7}\{\left|\hat{H}_j(k)\right|\}, 0 \le k \le N-1 \tag{19}$$

5 Numerical Results and Discussion

In this section, we show some simulation results for the proposed BEM based channel estimation and ICI mitigation. Here the parameters of the OFDM systems are as follows: the total number of the subcarriers N is 256 and cyclic prefix P is 16 in one sub-OFDM symbol. The length of cyclic prefix is larger than the maximum path delay. We have $M = 16$ equidistant

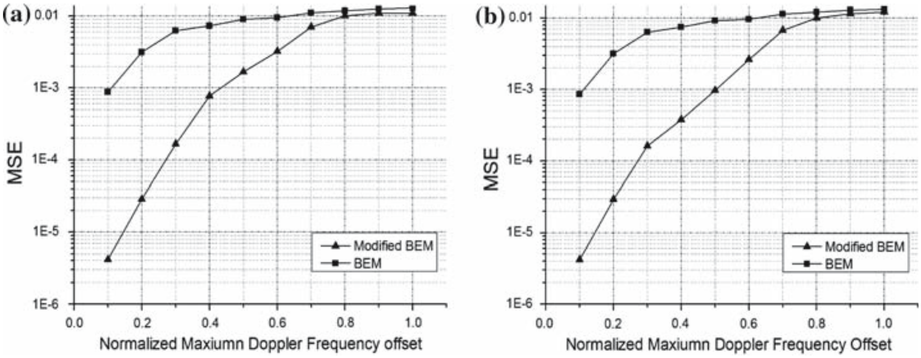

Fig. 3 (**a**) The simulated channel by BEM and Modified BEM $K_1 = 272$; (**b**) The simulated channel by BEM and Modified BEM $K_2 = 816$

pilot clusters, each containing $L_P = 6$ pilot subcarriers. In every pilot cluster, we set the second and fifth subcarrier to be the pilot data and the other to be the guard subcarriers. A six-path double selective channel generated by Jake's model is selected. The carrier frequency f_C is 5 GHz and the sample time T_S is 0.8 μ s (QPSK modulation). The maximum Doppler frequency $f_{\max} = v f_C / c$, where v indexes the mobile receiver velocity and c the speed of light, determines the variation of the channel. We normalize $f_{\max}$ in one sub-OFDM symbol by multiplying N and T_S. In all these situations, $Q = 2$ is enough to build a double selective channel by the modified BEM model as in (1) in respect that $f_{\max} K T_S$ is below one.

5.1 Simulation for Modified Channel Model

The first simulation will address the accuracy comparison between the Basis Expansion Model of [6] and our modified model. We use the mean square error to evaluate the performance. Here $h_J(m, l)$ is the simulated channel generated by Jake's model and $\bar{h}(m, l)$ is the channel rebuild by the two Basis Expansion Models described in Sect. 2.

$$MSE = \frac{1}{N} \sum_{m=0}^{N-1} \sum_{l=0}^{L-1} \left| h_J(m, l) - \bar{h}(m, l) \right|^2 \tag{20}$$

We compare the channel model for two BEM window lengths, which are $K_1 = 272$ (the sub-block length with CP) and $K_2 = 816$ (the block length). In order to be same with the channel estimation method discussed in Sect. 3, we divide every BEM window in $Q+1$ groups and use the average time domain channel impulse response of every group to regenerate the double selective channels. All the time domain channel impulse responses are generated by Jake's model. For the purpose of comparison, we select the different normalized $f_d = f_{\max} K T_S$ with K_1 and K_2. Since our modified BEM operates for f_d is below one, the simulation range of f_d is from 0.1 to 1.0.

Figure 3a and 3b shows the MSE of the BEM and modified BEM with the perfect time domain channel impulse responses. The results show that the modified BEM can approximate the double selective channels more accurately for small f_d. When f_d gets close to "1", the performances of two model are nearly the same. Besides, the key factor which influences the channel rebuild performance is f_d. With the different window length, we can achieve similar performance if f_d is the same.

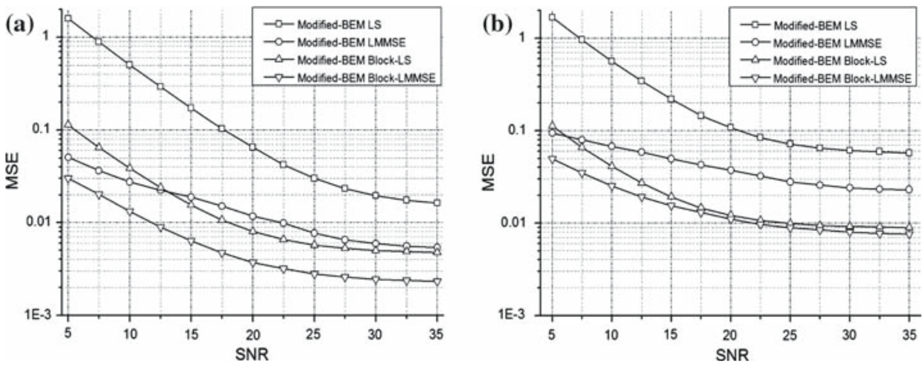

Fig. 4 (**a**) The simulated channel estimation performances v=100 $km/h f_{\max} NT_S$=0.0948; (**b**) The simulated channel estimation performances v=200 $km/h f_{\max} NT_S$=0.1896

5.2 Simulation for Channel Estimation

The second simulation addresses the analysis of the proposed modified BEM channel estimation based on block transmission. We compared our block type channel estimation algorithm with the algorithm proposed in [11] by simulations. To be fair, the channel model used in [11] has been replaced by the modified BEM. Two types of double selective channels are selected: (i) $f_{d1} = 0.0948$, (ii) $f_{d2} = 0.1896$. We also use mean square error (MSE) in (20) to evaluate the performance, only replace the $\bar{h}(m, l)$ with the channel estimation result based on modified BEM described in Sect. 2. Figure 4a and b show the MSE performance of the proposed channel estimation for different Doppler effects. Here we use $Q + 1 = 3$ basis to rebuild the channel with the modified BEM (4). The results show that we can improve the performance of the original algorithm in [11] both in the high and low SNR regime. There the matrix $\boldsymbol{\Xi}$ in (10) and (11) is full rank. With the support of $Q + 1$ sub-OFDM symbols as well as the modified BEM model, the method can rebuild the double-selective channel more accurately when $f_{\max} K T_S < 1$.

5.3 Simulation for ICI Cancellation

The effect of the ICI cancellation based on the two types of phase compensation for the block transmission OFDM system is examined next. Figure 5 shows the BER performances, for which f_d equals to 0.0948, 0.1896 and 0.284. It can be easily observed that the combined phase compensation algorithm significantly improves the system performance. Figure 6 shows the bit error ratio (BER) for "*CP*" and "*CH*" based cancellation with $\tilde{\mathbf{D}}_{CP}$ and $\tilde{\mathbf{D}}_{CH}$, individually. As can be seen, both the $\tilde{\mathbf{D}}_{CP}$ from consistent carrier frequency offset hypothesis and the $\tilde{\mathbf{D}}_{CH}$ from BEM channel estimation can improve the system performance. Obviously, the combined structure can provide further improvement over the single type of the phase compensation matrix.

5.4 Complexity Analysis

The complexity is evaluated in terms of the amount of computations needed for the algorithms, including both the required storage and the computational complexity. Referring to Sect. 3, we consider the complexity of both the channel estimation and the ICI cancellation.

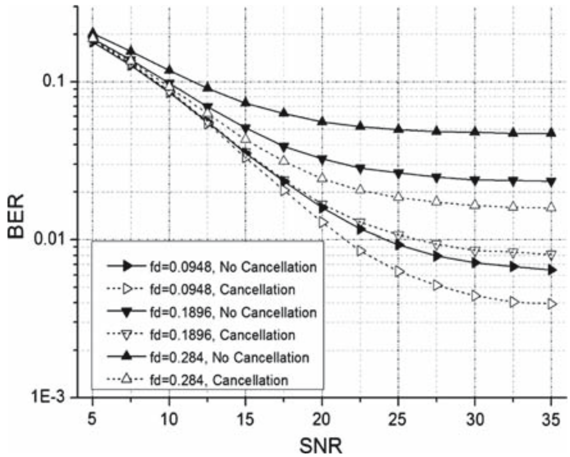

Fig. 5 Performances of combined ICI cancellation

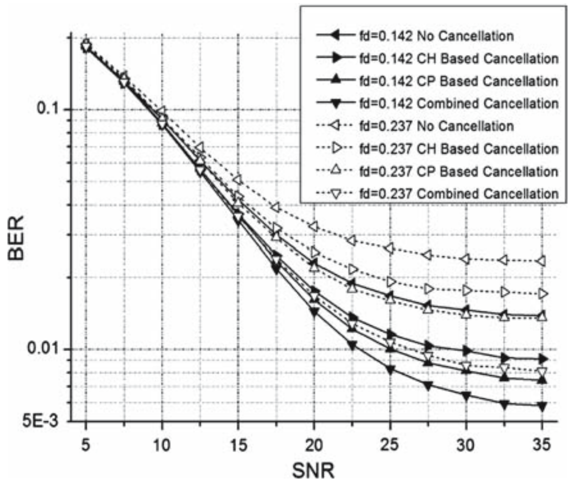

Fig. 6 Performances of different compensation matrices

For the channel estimation part, the calculation of $\hat{\mathbf{h}}_{LS}$ and $\hat{\mathbf{h}}_{LMMSE}$ does not need much computation because of the small sizes of the matrices $\boldsymbol{\Xi}$ and $\boldsymbol{\Psi}$ (The size of $\boldsymbol{\Xi}$ and $\boldsymbol{\Psi}$ is $M(Q+1)(L_P - B_C) \times (Q+1)(L+1))$). For the ICI cancellation part, the dimension of the FFT in stage 3 dominates the complexity. To obtain one group of rotary optional demodulation coefficients such as $\hat{\mathbf{H}}_j$, one N-length and one M-length FFT are required, which require $N\log_2(N)$ and $M\log_2(M)$ complex valued multiplications in one sub-OFDM symbol, respectively. To obtain the best demodulation coefficients $\hat{\mathbf{H}}_{j(\max)}$ from all optional $\hat{\mathbf{H}}_j$, eight N-length and M-length FFTs and a storage capacity with the length of $8N$ are needed. In other words, the implementation of the new receiver will not add much burden to the total computational calculation.

6 Conclusions

In this paper, we have proposed a modified Basis Expansion Model (BEM), which is more accurate than the original BEM for double-selective channels when the normalized maximum Doppler frequency is below one. Then based on this model, the block type OFDM channel estimation and the ICI cancellation algorithm are presented. By applying the BEM based channel estimation, we can obtain more accurate channel information both in lower and higher SNR situations. With the combination of the phase compensation and the demodulation, we can reduce the ICI caused by time-variant channels and improve the BER performance of the systems effectively.

Acknowledgement This work was supported in part by Chinese Government Scholarship Program (CGSP).

References

1. Weinstein, S. B., & Ebert, P. M. (1971). Data transmission by frequency division multiplexing using the discrete Fourier transform. *IEEE Transactions and Communications, 19*, 628–634.
2. Jeon, W. G., Chang, K. H., & Cho, Y. S. (1999). An equalization technique for orthogonal frequency division multiplexing systems in time-variant multipath channels. *IEEE Transactions and Communications, 47*, 27–32.
3. Schniter, P. (2004). Low-complexity equalization of OFDM in doubly selective channels. *IEEE Transactions on Signal Process, 52*, 1002–1011.
4. Barhumia, I., Leusb, G., & Moonen, M. (2005). Time-varying FIR equalization for doubly selective channels. *IEEE Transactions on Wireless Communications, 4*, 202–214.
5. Hou, W., & Chen, B. (2005). ICI cancellation for OFDM communication systems in time-varying multipath fading channels. *IEEE Transactions on Wireless Communications, 4*(5).
6. Giannakis, G. B., & Tepedelenlioglu, C. (1998). Basis expansion models and diversity techniques for blind identification and equalization of time-varying channels. *Proceedings of IEEE, 86*, 1969–1986.
7. Ma, X., Giannakis, G. B., & Shuichi Ohno. (2003). Optimal training for block transmissions over doubly selective wireless fading channels. *IEEE Transactions on Signal Process, 51*(5), 1351–1366.
8. Jakes, W. C. (1994). *Microwave mobile communications*. New York: *IEEE Press*.
9. Bhashyam, S., Sayeed, A. M., & Aazhang, B. (2000). Time-selective signaling and reception for communication over multipath fading channels. *IEEE Transactions and Communications, 48*, 83–94.
10. Sayeed, A. M., & Aazhang, B. (1999). Joint multipath-doppler diversity inmobile wireless communications. *IEEE Transactions and Communications, 47*, 123–132.
11. Tang, Z., Leus, G., Cannizzaro, R. C., & Banelli, P. (2006). Pilot Assisted Time-Varying OFDM Channel Estimation. *ICASSP*. vol. 4, May 2006.
12. Jeruchim, M. C., Balaban, P., & Shanmugan, K. S. (1992). *Simulation of communication systems*. New York: Plenum Press.
13. Bhashyam, S., Sayeed, A. M., & Aazhang, B. (2000). Time-selective signaling and reception for communication over multipath fading channels. *IEEE Transactions on Communications, 48*, 83–94.
14. Viterbo, E., & Boutros, J. (1999). A universal lattice code decoder for fading channels. *IEEE Transactions on Information Theory, 45*, 1639–1642.
15. Ma, X., & Giannakis, G. B. (2003). Maximum-diversity transmissions over doubly selective wireless channels. *IEEE Transactions on Information Theory, 49*, 1832–1840.
16. Coleri, S., Ergen, M., Puri, A., & Bahai, A. (2002). Channel estimation techniques based on pilot arrangement in OFDM systems. *IEEE Transactions on Broadcasting, 48*(3), 223–229.
17. Qiao, Y., Yu, S., Su, P., & Zhang, L. (2005). Research on an iterative algorithm of LS channel estimation in MIMO OFDM systems. *IEEE Transactions on Broadcasting, 51*(1), 149–153.
18. Yang, B., Cao, Z., & Letaief, K. B. (2001). Analysis of low-complexity windowed DFT-based MMSE channel estimator for OFDM systems. *IEEE Transactions and Communicatons, 49*(11).
19. Beek, J., Sandell, M., & Börjesson, P. O. (1997). ML Estimation of time and frequency offset in OFDM Systems. *IEEE Transactions on Signal Process, 45*(7).

Author Biographies

Qi Jiang received the B.E. and M.E. degrees in Communications Engineering from Southeast University, Nanjing, P.R. China, in 2003 and 2005, respectively. He is currently pursuing the Ph.D. degree at the National Mobile Communications Research Lab., Southeast University. From Nov. 2006 to Nov. 2007, he is with the Institute of Telecommunications as a visiting researcher, University Stuttgart, German. His current interests are in the areas of signal processing in communication, wireless communications, communications over time- and frequency-selective channels, equalization, and synchronization.

Joachim Speidel studied Electrical Engineering and Information Technology at the University of Stuttgart, Germany, and received his Dipl.-Ing. and Dr.-Ing. degrees in 1975 and 1980, respectively, all *summa cum laude*. From 1980 to 1992 he worked for Philips Communications (today Lucent Technologies Bell Labs Innovations, Germany) in the field of digital communications, ISDN and video communications. During his industry career he has held various positions in R&D, as a member of technical staff, laboratory head and finally as Vice President. Since autumn 1992 he has been Full Professor at the University of Stuttgart and Head of the Institute of Telecommunications. His research areas are digital multimedia communications in mobile, optical and electrical networks with emphasis on modulation, source and channel coding.

Chunming Zhao received the B.S. and M.S. degrees from Nanjing Institute of Posts and Telecommunications, in 1982 and 1984 respectively. In 1993, he received his Ph.D. degree from the Department of Electrical and Electronic Engineering, University of Kaiserslautern, Germany. He has been a Postdoctoral Researcher at National Mobile Communications Research Lab., Southeast University, where he is currently a professor and vice director of the Lab. He has managed several key projects of Chinese Communications High Tech. Program and was awarded as "excellent researcher" form Ministry of Science and Technology, China. His research interests include communication theory, coding/decoding algorithms, mobile communication, adaptive filtering and VLSI design.